Cite this article
Chi SY, Liu CJ, Tan CH and Chen YH
Study of typhoon impacts on the foundation design of offshore wind turbines in Taiwan.
Proceedings of the Institution of Civil Engineers – Forensic Engineering,
https://doi.org/10.1680/jfoen.19.00011

Research Article
Paper 1900011
Received 16/09/2019; Accepted 23/04/2020

Keywords: foundations/offshore engineering/steel structures

Forensic Engineering

ice Publishing

Study of typhoon impacts on the foundation design of offshore wind turbines in Taiwan

Shu-Yung Chi PhD
Director, Geotechnical Engineering Research Center, Sinotech Engineering Consultants, Inc., Taipei, Taiwan (corresponding author: sychi@sinotech.org.tw)

Che-Jen Liu MPhil
Senior Researcher, Geotechnical Engineering Research Center, Sinotech Engineering Consultants, Inc., Taipei, Taiwan

Chih-Hao Tan PhD
Senior Principal Researcher, Geotechnical Engineering Research Center, Sinotech Engineering Consultants, Inc., Taipei, Taiwan

Yi-Hsuan Chen MPhil
Senior Researcher, Geotechnical Engineering Research Center, Sinotech Engineering Consultants, Inc., Taipei, Taiwan

Taiwan is hit by an annual average of three to four typhoons with different intensities and routes. To consider the impacts of typhoon events on offshore substructure design, the historical metocean data for storm event-based frequency analysis are generally applied. However, whether a supertyphoon passes directly over an offshore wind farm has a great influence on the results of frequency analysis. Therefore, the American Bureau of Shipping has recently increased the return period of hydrodynamic loads from 50 to 100 years to address the higher variation in the severity of extreme storms in typhoon-prone offshore regions. In this paper, to assess the impacts of the increase in the return period (from 50 to 100 years) on the design of offshore substructures, case studies of different types of substructures (i.e. monopile, three-leg jacket and four-leg jacket) with different water depths were conducted for the offshore wind farms off the coast of Changhua County in central Taiwan. The quantitative differences in foundation design are presented by way of a comparison of substructure weights, overturning moments and pile lengths. The preliminary results of the case studies show that the monopile design is more obviously dominated by earthquakes than by typhoons and the jacket-type foundation is more significantly dominated by typhoons.

Notation

A_{475}	seismic load with a 475-year return period
E_{100}	environmental load with a 100-year return period
E_{50}	environmental load with a 50-year return period
E_{n}	environmental load in the normal state
F_{xf}	horizontal force in the x-axis direction
G	permanent load
$H_{\max}$	maximum wave height
H_{s}	significant wave height
$\mathrm{LC}_{\mathrm{eqk}}$	load combination for an earthquake
$\mathrm{LC}_{\mathrm{ftg}}$	load combination for fatigue
$\mathrm{LC}_{\mathrm{storm\ I}}$	load combination for extreme storm I with unfavourable permanent loads
$\mathrm{LC}_{\mathrm{storm\ II}}$	load combination for extreme storm II with favourable permanent loads
M_{yf}	horizontal moment in the y-axis direction
M_{zf}	vertical moment
T_{p}	peak period of a wave
v_{r}	known wind speed at the reference height z_{r}
v_z	wind speed at height z above sea level

1. Introduction

The government of Taiwan is focused on promoting offshore wind energy. By the end of 2017, 18 potential offshore wind farms with a total of 10.5 GW of capacity had passed Taiwan's environmental impact assessment process, and ten of them, with 5.5 GW of grid capacity, will be connected to the grid by 2025. This means that business opportunities in offshore wind power will continue for many years in Taiwan.

However, Taiwan is located in the low latitudes of the western North Pacific, and it is usually hit by typhoons in summer and autumn, with an average of three to four times annually. Typhoons can have significant impacts on offshore wind farms. In addition, it should be also considered that, due to climate change, the average sea level is rising year by year due to increases in ocean temperature. According to the Fifth Assessment Report of the Intergovernmental Panel on Climate Change (IPCC), for the most conservative scenario (RCP8.5), the global mean sea level will rise by 0.52–0.98 m by the year 2100 and at a rate of 8 to 16 mm/year during 2081–2100 (Stocker *et al.*, 2013). Based on the IPCC's scenario simulations, it can also be estimated that the mean sea level in the Taiwan Strait will rise by around 0.2 m during 2020–2050. In designing a wind farm development that ensures safety and cost simultaneously, meteorological and oceanographic (metocean) data play an important role. The key to the successful development of an offshore wind farm is whether the collected metocean data are sufficient to reflect the complex environmental conditions during the entire life cycle of an offshore wind farm, from site screening, feasibility study, planning and design to construction, installation, operation, maintenance and decommissioning. The developers need to consider the uncertainties and risks of natural hazards and extreme climate conditions.

At present, the guidelines and standards suggested by the International Electrotechnical Commission and Det Norske Veritas & Germanischer Lloyd, mainly based on the European experience of developing offshore wind farms in the North Sea, are widely used internationally for the foundation designs of offshore wind turbine generators (WTGs). Based on the European experience, for extreme environmental conditions, according to the standards for offshore structures, the 50-year return period is usually adopted for offshore foundation design (DNV GL, 2016a; IEC, 2005). However, other series of standards and guidelines have been suggested by the American Petroleum Institute (API) and International Organization for Standardization based chiefly on the American experience of offshore petroleum exploitation, particularly in the Gulf of Mexico. These standards and guidelines adopt the 100-year return period as the extreme conditions for offshore substructure design. In particular, after Hurricane Katrina (2005), which caused extensive damage to offshore petroleum platforms in the Gulf of Mexico, the American Bureau of Shipping (ABS) conducted a series of research studies of tropical cyclones in the Gulf of Mexico. The results of dropsonde measurement, for example, indicate that the measured average wind speed of the wind speed profile of tropical cyclones is obviously higher than the exponential profile of the extreme wind speed model with a 50-year return period of wind speed recommended by IEC 61400-1 (IEC, 2005), and the measured profile is also steeper than the logarithmic curve of the wind profile suggested by API RP 2MET (API, 2014a). Therefore, the latest edition of the ABS guidelines recommends the adoption of the 100-year return period as the extreme conditions for offshore structure design (ABS, 2018).

It is urgent for the developers of offshore wind farms in the Taiwan Strait to clarify whether the traditional design standards using the 50-year return period as the extreme conditions in the 20-year life cycle of offshore wind farms can fully cover the possible metocean risks. Although much research has been conducted to compare the parametric differences of metocean data between the 50- and 100-year return periods, a few case studies have conducted quantitative research with different environmental conditions for the design of offshore structures.

In this paper, WTG foundation designs were compared under different conditions – namely, two return periods (50 and 100 years), three water depths (from 27.5 to 45 m) and three foundation types (i.e. monopole, three-leg jacket and four-leg jacket) – for the littoral area off the coast of Changhua County in central Taiwan. The results focus on the weights of the structures, the overturning moments and the length of the piles. The results can be used as a preliminary reference for the development of offshore wind farms in Taiwan and could provide developers with a better understanding of typhoon impacts and countermeasures.

2. Frequency of typhoon impacts

Taiwan is frequently hit by typhoons, and a total of 366 typhoons affected the island from 1911 to 2018 (CWB, 2019). Predictably, the values of metocean parameters determined from the long-term measured data in the Taiwan Strait are generally higher than the values based on the measured data in the North Sea. For example, the wave height for the presented case in the Taiwan Strait is 17.75 m for the 27.5 m water depth condition, which is significantly higher than the wave height of 9.5 m under a similar condition (25 m water depth) for the London Array offshore wind farm in the North Sea.

Hence, under such severe metocean conditions, the designs of the outer diameter and thickness of offshore structural members need to be increased effectively to resist the shear forces and bending moments resulting from the environmental loads. When offshore structural members are larger, the offshore structure will be subjected to larger environmental loads. In other words, for the stability of a WTG support structure, there is quite a large overturning moment at the level of the seabed due to lateral hydrodynamic loadings, so structural members of larger diameters and longer piles are required to resist the overturning moment of a monopile foundation or to resist the induced axial forces of a jacket foundation.

Regarding the paths of typhoons, wind speeds, wave heights and storm surges are higher when typhoons directly pass over wind farms than when typhoons pass by the wind farms. Taiwan's Central Weather Bureau has analysed the statistical data on the paths of typhoons that hit Taiwan from 1911 to 2017 and grouped the paths of typhoons into ten categories. The probability of the occurrence of each category is shown in Figure 1 (CWB, 2019). However, regardless of which method of frequency analysis (e.g. the annual maximum method or the peak-over-threshold method)

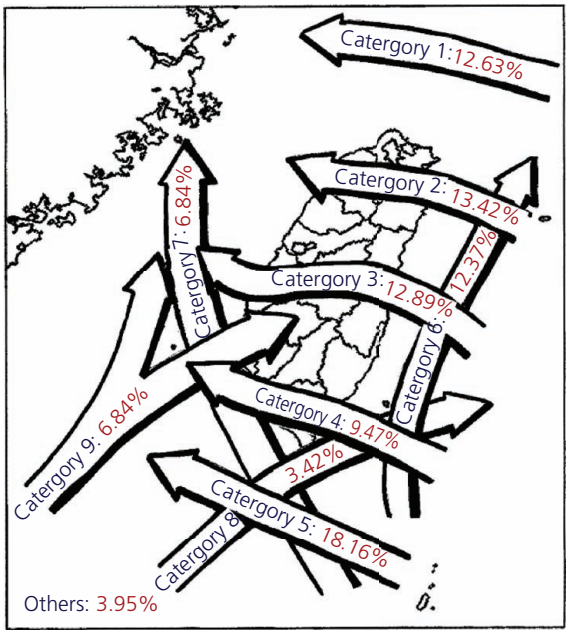

Figure 1. Diagram of categorised paths of typhoons striking Taiwan between 1911 and 2018 (CWB, 2019)

is adopted, the observed metocean data of typhoons that pass far away from the wind farms are still sampled in the statistical analysis, so the values of metocean design parameters might be underestimated. Therefore, this study calculated and compared the design values of the 50-year return period suggested by the European standards (e.g. DNVGL-ST-0126 (DNV GL, 2016a) and DNVGL-ST-0437 (DNV GL, 2016b)) and those of the 100-year return period suggested by the American standards (e.g. API RP 2MET (API, 2014a)) to clarify whether the adoption of the 50-year return period is sufficient to consider the effects of typhoons on offshore foundation design in Taiwan.

3. Design parameters

3.1 Metocean data

Many metocean parameters should be considered in the offshore substructure design, some examples being water depth, wave height, current velocity, splash zone height and marine growth. Based on the deeper water depth in the Taiwan Strait for considering the offshore wind farm development in the next stage, water depths of 27.5, 35.0 and 45 m were adopted for the case studies of the offshore structural analysis. Other key metocean parameters used in the case studies are listed as follows.

3.1.1 Water level

The water level was considered as the mean tide level, the highest high-water level, the storm surge and the sea level rise caused by climate change. The vertical datum of the orthometric height system is Taiwan Vertical Datum (TWVD) 2001. The design water levels for different return periods are listed in Table 1.

Table 1. Design water levels

Item	Water level: m TWVD
Mean water level	+0.310
1-year design high-water level	+4.316
50-year design high-water level	+4.956
100-year design high-water level	+5.136

Table 2. Design wave heights

Depth: m	Item	Wave characteristics
27.5	1-year H_{max}: m	13.20
	1-year T_p: s	10.96
	50-year H_{max}: m	17.75
	50-year T_p: s	13.30
	100-year H_{max}: m	19.98
	100-year T_p: s	14.11
35.0	1-year H_{max}: m	13.20
	1-year T_p: s	10.96
	50-year H_{max}: m	17.91
	50-year T_p: s	13.36
	100-year H_{max}: m	20.21
	100-year T_p: s	14.20
45.0	1-year H_{max}: m	13.20
	1-year T_p : s	10.96
	50-year H_{max}: m	18.44
	50-year T_p : s	13.56
	100-year H_{max}: m	20.76
	100-year T_p : s	14.38

3.1.2 Wave height

The design wave height, estimated from the conditions of water depth in the Taiwan Strait, was used to conduct the ultimate limit state (ULS) analysis, as listed in Table 2, in which H_{max} means the maximum wave height and T_p means the wave period corresponding to H_{max}. In addition, the joint probability distribution of a significant wave height (H_s) and a peak period (T_p), as shown in Figure 2, was used to conduct the spectral-based fatigue analysis, and the Joint North Sea Wave Project wave spectrum was adopted to simulate the random behaviour of waves.

3.1.3 Currents

Table 3 lists the current velocities for different return periods. It was conservatively assumed that the currents would flow in the same direction as the waves. In addition, the contribution of currents to cyclic loads on the structures was assumed to be slight, so the current effects on the fatigue analysis were ignored.

3.1.4 Splash zone, marine growth and corrosion allowance

The splash zone is a vulnerable area of an offshore structure that faces corrosion from severe environmental conditions such as the atmosphere, waves and currents. In this study, the range of the

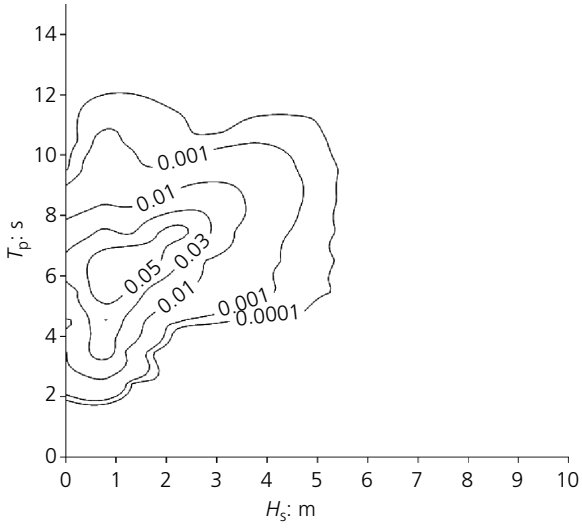

Figure 2. Joint occurrence distribution of significant wave height and peak period. Note: the white area in the figure denotes no drilling data

Table 3. Design current speeds

Return period: years	Design current speed: m/s
1	1.156
50	2.673
100	2.832

splash zone was −6.00 to +8.93 m (in TWVD), determined from the related standard DNVGL-RP-0416 (DNV GL, 2016c).

Regarding marine growth, which leads to increased wave loads on the structure, the thickness of marine growth was assumed to vary with water depth. For example, for depths of 10 m or less below the water surface, the thickness was 20 cm, and for depths greater than 10 m, the thickness was 10 cm. The density of marine growth was assumed 1.4 t/m^3.

The corrosion allowance is the additional material thickness to allow for metal loss caused by environmental corrosion while still maintaining the design strength of the structural members during the design life. The corrosion allowance was also estimated according to the related standard DNVGL-RP-0416 (DNV GL, 2016c). The total thickness of the corrosion was assumed 0.4 cm during the design life, and the corrosion allowance was specified to be 0.3 cm within 2 m above the seabed to consider the effect of microbiological corrosion.

3.1.5 Wind force

Instead of the wind force applied directly to the rotor and the tower, this study adopted the equivalent force at the interface between the tower and the substructure, which was provided by the wind turbine supplier, to design the substructures. Furthermore, only the 50-year return period data were available, so the 100-year return period equivalent interface force, regarded as the design condition, was estimated in the study by the following simplified procedures. To start with, the normal shutdown situation of the wind turbine was considered, and a structural model was adopted to build a simplified rectangle to simulate the area of the complicated shape of the rotor and nacelle assembly (RNA). Next, the size and the centre position of the rectangle of the model were modified and the 50-year return period wind force was applied to the rectangle and the tower repeatedly until the results of structural static analysis showed that the calculated interface force was equal to the interface force provided by the wind turbine supplier. Finally, the 100-year wind force was applied to the rectangle of the calibrated model to obtain the 100-year return period equivalent interface force. In the aforementioned procedures, the wind speed condition was based on a height of 90 m (in TWVD), a 10 min average wind speed of 60.9 (m/s) and a 100-year wind speed of 65.4 (m/s). The wind profile was assumed to satisfy the following relationship:

$$v_z = v_r \left(\frac{z}{z_r}\right)^{1/10} \quad (1)$$

3.2 Condition of the wind turbine

For the conceptual design of the substructure of the offshore wind turbine, the supplier of the wind turbine should provide the key parameters, including the weight of the RNA, the elevation of the hub, the allowable range of the natural period of the WTG and the forces at the interface between the tower and the substructure for ULS and fatigue limit state (FLS) analyses. For the ULS analysis, the supplier of WTGs performs the integrated simulations and calculations according to the design situations and load cases listed in IEC 61400-3 (IEC, 2009) and obtains the results of the worst case for the design wind conditions in the normal operation situation of power production. Thus, the forces at the interface between the tower and the substructure for ULS analysis can be obtained.

For the FLS analysis, the WTG supplier selects cases related to FLS based on the results of integrated simulations and then sets up the load-time series at the interface in accordance with the occurrence probability of each case for the whole life cycle of a WTG. Based on the rainflow-counting method (ASTM, 2011) with the load-time series, the number of cycles against the difference in interface stress ranges can be determined. Finally, under the same fatigue damage conditions, the equivalent load against 10^7 cycles can be obtained from the appropriate S–N curve.

An 8.0 MW wind turbine was adopted to carry out the substructure design of wind turbines, and its relevant parameters are summarised in Table 4. Because only the equivalent loads for a 50-year return period were derived from the integrated simulations and provided by the wind turbine supplier, this study assumed that the equivalent load for a 100-year return period could be calculated as the design wind speed for a 100-year return period multiplied by the equivalent rectangular area of the rotor and nacelle, which was back-calculated from the design wind speed for a 50-year return period. The calculated equivalent loads at the interface between the tower and the substructure are listed in Table 5.

3.3 Soil condition

This paper refers to the offshore geological drilling data for a location off the coast of Changhua County in central Taiwan, as shown in Figure 3. The strata can be divided into three layers of cohesionless soils (sand or silt) and two layers of cohesive soils (clay or silty clay) within a depth of 80 m, and the shallow layers mostly consist of sandy soils. The static and weakened p–y and t–z curves of the shallow layers were established using the API RP 2GEO standard (API, 2014b: pp. 32–40). The study

Table 4. Wind turbine parameters

Output power: MW	8
Hub elevation: m TWVD	109
Tower/foundation interface: m TWVD	19
RNA mass: t	482.3
Bandwidth of eigenperiod: s	3.831–5.208

Table 5. Equivalent loads at the interface between the tower and the substructure

Load condition	50-year ULS	100-year ULS	ULS in operation	FLS
F_{xf}: kN	2808	3238	1600	860
M_{yf}: kN m	250 045	288 364	156 687	50 870
M_{zf}: kN m	5515	6360	−751	14 810

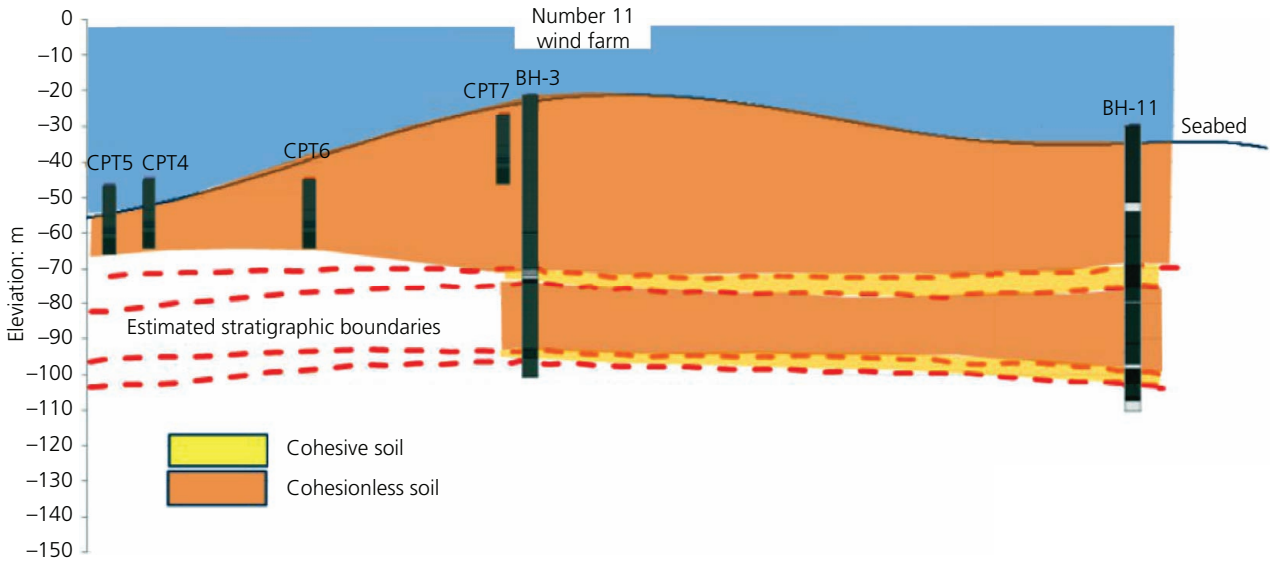

Figure 3. Geological profile identification diagram for the offshore area of Changhua County (see F3WP PO, 2018)

considered only the lateral displacement of the soil under the cyclic loadings and adopted the static soil parameters with safety factors to determine the pile length based on practical design experience (API RE 2GEO (API, 2014b: p. 103)). For the strength of liquefied soil induced by a large earthquake, no lateral resistance within a depth of 20 m of liquefied soil below the seabed was assumed in the study.

3.4 Earthquake design

The horizontal acceleration response spectrum for a 475-year return period was adopted to consider the effects of earthquakes on the design in the study (DNVGL-ST-0437 (DNV GL, 2016b: p. 47)). The loadings induced by earthquakes, emergency shutdown of the wind turbine and the normal sea state were superposed under the earthquake situation. In addition, a damping ratio of 5% was used in dynamic analysis with soil liquefaction analysis. The vertical acceleration was assumed to be 0.3 times the horizontal acceleration. The horizontal acceleration response spectrum for a 475-year return period is shown in Figure 4.

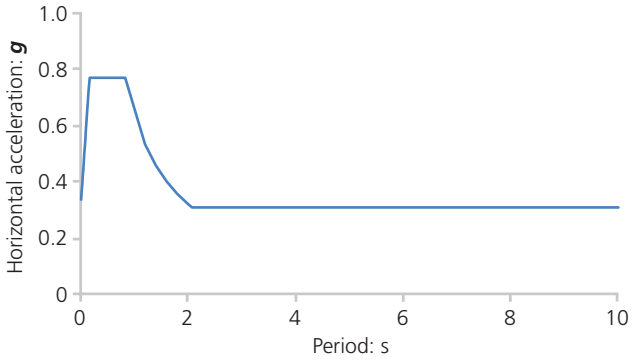

Figure 4. Designed response spectrum for a 475-year return period (see F3WP PO, 2018)

4. Methodology

4.1 Basic assumptions

The overall structures of the offshore wind turbine are shown in Figure 5. The RNA, the tower and their relevant design parameters were developed and provided by the WTG supplier. The substructure refers to a jacket-type or a monopile-type foundation, which is the scope of this study. The basic assumptions for the design of the substructure are as follows.

- The wall thickness transition section is designed inside the tubular member.
- A minimum diameter/thickness ratio of 20 is assumed.
- The lifting capacity is not considered in the design.
- A service life of 20 years is assumed for substructures, and fatigue due to pile driving and transportation is not considered.
- Only the primary steel is designed in this study, and the influence of the secondary steel on the primary steel is not considered.

4.2 Design process

The design process (shown in Figure 6) of an offshore wind turbine substructure includes numerous code checks and iteration steps. The Sacs software, developed by Bentley, is used for the finite-element analysis of a beam-element model. It has the capabilities of two-dimensional (2D) hydrodynamic simulation, empirical wind force calculation and consideration of the non-linear pile–soil interaction in the structural analysis. Only the global model is analysed, and the associated model parameters are referenced from the standards or best practice in the industry. The

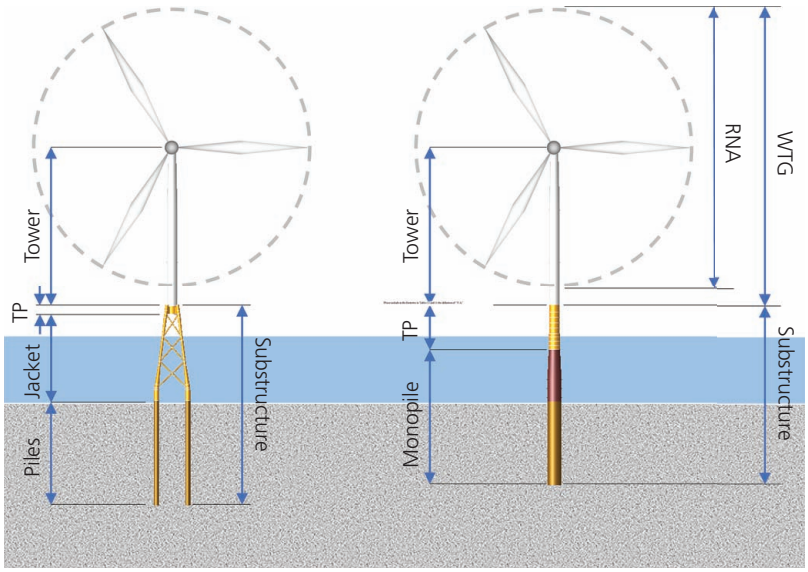

Figure 5. Diagram of offshore WTG substructures: TP, transition piece

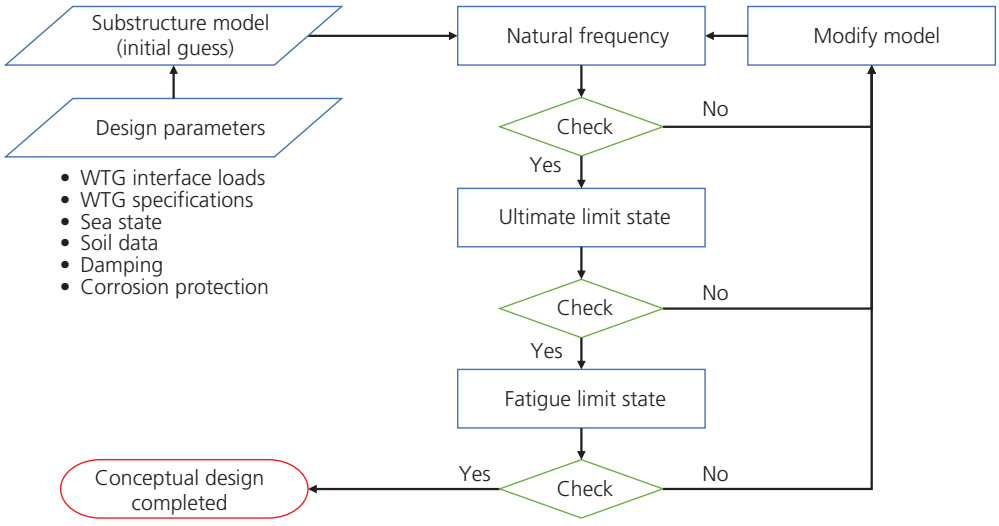

Figure 6. Design flow chart for an offshore WTG substructure

global model includes all the wind turbine structures, such as the RNA, the tower and the substructure, which includes the embedded pile. However, the RNA is modelled from a mass point rather than the beam elements.

4.2.1 Geotechnical and hydraulic design

The geotechnical design includes the assessment of soil strength and the design of the piles, and the hydraulic design includes calculation of the hydraulic loads based on the preliminary member size with subsequent modification of the member size according to the calculated results. Any modification changes the hydraulic loads, leading to an iterative process.

4.2.2 Natural period check

The natural period of a wind turbine structure must meet the requirement that the period of the first mode shape is within the allowable range provided by the WTG supplier and is determined by considering the 1P and 3P periods of the structure. An 8 MW WTG is applied, and its allowable range is 3.831–5.208 s.

4.2.3 ULS analysis and check

In the ULS, 50- and 100-year return periods are considered for storms and a 475-year return period is applied for earthquakes. The corrosion allowance is 100% depletion. In the analysis of storm-type load combinations, the velocity and the acceleration

field in water are solved by a 2D hydrodynamic module, and then the hydraulic loads are determined by the Morison equations. The loads from the RNA and the action of wind on the tower are applied as the equivalent loads provided by the WTG supplier on the interface between the tower and the transition piece. However, in the analysis of earthquake-type load combinations, the spectral earthquake analysis method is applied, and the structural response is calculated in the deflection driven system, in which all pile heads are assumed to move with the ground motion. After the structural response of each mode shape is derived, a complete quadratic combination is used to combine all the mode shape results, and then the equivalent static loads can be derived. Furthermore, the loads due to emergency shutdown from the WTG and the loads resulting from the normal sea state are all combined with the equivalent static loads for further static analysis. After the inner forces of all members are derived, the unity ratio of axial force, bending moment, shear force and buckling is checked in accordance with the NORSOK N-004 standard (Standards Norway, 2013). All utilisation ratios must be less than 1.0. For the design of the embedded piles, the safety factor for the axial bearing of a jacket pile must be greater than 1.30, while the embedded pile length of a monopile must be greater than the critical pile length, at which the change in rotation over a 2 m increment introduces a less than 1.0% decrease in pile head rotation relative to the pile head rotation for an excessively long pile.

4.2.4 FLS analysis and check

The fatigue due to wind and waves is considered, and Miner's rule is applied to cumulate the fatigue damages. For wind-induced fatigue, deterministic fatigue analysis is used. The hot spot stress range is derived from two wind loads, and then the number of cycles to failure can be obtained in the corresponding hot spot *S–N* curve. The fatigue damage is the given number of stress cycles divided by the number of cycles to failure. For wave-induced fatigue, spectral fatigue analysis is used. The method assumes that there is a definable relation between wave height and stress ranges at the connections and that at any point the elevation of the sea above its mean value is a stationary Gaussian random process. When the stress range is a Rayleigh-distributed random variable, the expected damage can be derived from a wave spectrum and a transfer function with the corresponding hot spot *S–N* curve. The design cumulative damage is the sum of wind-induced and wave-induced fatigue damage multiplied by the safety factor, and it must be less than 1.0. Moreover, in the case of fatigue analysis, 50% corrosion allowance is considered, and the stress concentration factors and the *S–N* curves refer to the recommended practice DNVGL-RP-C203 (DNV GL, 2016d).

4.3 Load combinations

The load combinations refer to the DNVGL-ST-0437 standard and are shown as follows. For the jacket-type substructures, two additional horizontal orientations of loads are considered; 0 and 90° are considered in three-leg cases, while 0 and 45° are considered in four-leg cases

- extreme storm I with unfavourable permanent loads

2. $\mathrm{LC}_{\text{storm I}} = 1.1G + 1.35E_{50\text{ or }100}$

- extreme storm II with favourable permanent loads

3. $\mathrm{LC}_{\text{storm II}} = 0.9G + 1.35E_{50\text{ or }100}$

- earthquake

4. $\mathrm{LC}_{\text{eqk}} = 1.0G + 1.0E_{\text{n}} + 1.0A_{475}$

- fatigue

5. $\mathrm{LC}_{\text{ftg}} = 1.0G + 1.0E_{\text{n}}$

5. Results and discussion

5.1 Structural geometry

The individual structural members are designed with different wall thicknesses and outer diameters, and the perfect symmetry of the whole structure is maintained. For jacket-type substructures, the joint cans are thickened, the transition piece is in the form of plate girders connecting the tower bottom with the jacket legs and the pile heads are designed as grouted connections to combine a pile and a jacket leg together. For monopile-type substructures, the thickness design is applied on every can section with a height of 2–3 m, the grouted cone connection is used in the connection of a transition piece and a monopile, and the outer diameter of a monopile is increased in accordance with the grouted cone bevel to the designed maximum value. The general forms of the structural geometry are shown in Figure 7.

According to the aforementioned design methods and processes, the structural designs with 50- and 100-year return periods are completed and key geometrical parameters are shown in Tables 6–8. The geometry is designed to ensure that the natural period of the structure falls within the allowable range required by WTG suppliers, and the member size and thickness are intended to meet the design criteria under the ULS and the FLS conditions.

5.2 Natural period

The natural periods of the first mode shapes of the structures are shown in Figure 8. The periods of four-leg jackets are close to the lower bound of the allowable range. In general, the stiffness of a jacket is high, and to reduce the stiffness, the span of the adjacent piles is reduced. However, any abatement in the span will increase the pile axial loads, which are attributed to the tremendous overturning moment on the seabed. The balance between lowering stiffness and increasing pile axial loads must be

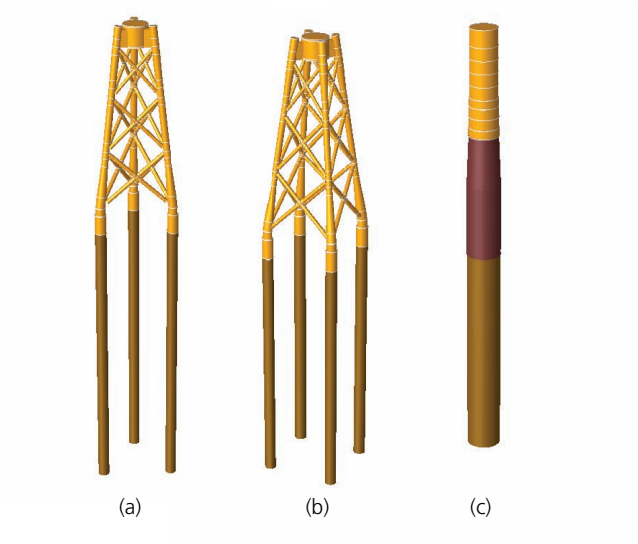

Figure 7. Geometry diagrams for the substructures of offshore WTGs: (a) three-leg jacket type; (b) four-leg jacket type; (c) monopile type

carefully maintained. The batters (refer to Figure 9) of the jacket legs for each case are listed in Tables 6 and 7.

5.3 Dominant load combination

The structural properties, such as thickness, outer diameter and member length, are determined by one of the load combinations. This means that the structural properties are controlled by the type of environmental loads, such as storms and earthquakes. Regarding a jacket-type substructure, not all members of the structure may be dominated by the same types of loads, so the numbers of members dominated by each type of loads are listed in Tables 9 and 10. For the 50-year storm cases, more than half of the structural members are dominated by earthquakes. When the return period of the storm is increased to 100 years, most of the structural members are dominated by storms instead. For monopile-type substructures, most of the can sections are dominated by earthquakes in the 50-year cases, but in the 100-year cases, all the sections are dominated by storms.

5.4 Utilisation ratio and fatigue

The utilisation ratio is defined as the ratio of structural response multiplied by the safety factor to the strength capacity and must be less than 1.0, according to design codes. The fatigue life must be greater than the design life. The uncertainty of loads and materials is considered in design codes. Designers can make utilisation ratios close to 1.0 and fatigue life approach the design life. However, additional safety margins may be taken into account in practice, so requirements exceeding the standards may be applied in projects.

Because the utilisation ratio and the fatigue life are closely related to the size and thickness of the structural members, their values should be designed within a suitable range to achieve a more consistent benchmark for comparison. The utilisation ratios and fatigue lives of all cases are shown in Tables 11 and 12. The maximum utilisation ratio of each case is within 0.85–0.90, and only in the case of jacket-type substructures can the fatigue lives fall between 20 and 30 years. The reason is that the joint cans of jackets can be thickened to overcome fatigue damage, whereas monopiles can only change the thickness evenly and gradually. When a monopile is dominated by the utilisation ratio, its thickness cannot be further reduced to decrease the fatigue life. On the other hand, if a monopile is dominated by the fatigue life, the maximum utilisation ratio will be below the benchmark range.

Table 6. Key parameters of the three-leg jacket-type substructures

Return period: years	50	50	50	100	100	100
Water depth: m	27.5	35	45	27.5	35	45
Diameter of TP: cm Wall thickness: cm	653 4.7	653 4.7	653 4.7	653 4.7	653 4.7	653 4.7
Cross-section of horizontal plate girder: cm × cm Wall thickness: cm	450 × 150 5.6	450 × 150 5.6	450 × 150 5.6	400 × 150 5.6	400 × 150 5.6	400 × 150 5.6
Number of brace layers	3	3	4	3	3	4
Jacket leg batter	11	8	8	11	8	8
Diameter of jacket leg: cm Wall thickness: cm	180–250 3.8–9.0	180–250 3.7–8.6	180–250 3.5–8.5	180–250 3.8–9.0	180–250 3.9–8.6	180–250 3.6–8.5
Diameter of brace: cm Wall thickness: cm	95–110 1.6–4.8	90–110 1.7–5.0	90–110 1.4–4.5	95–110 1.7–4.8	90–110 1.7–5.0	90–110 1.4–4.5
Diameter of embedded pile: cm Wall thickness: cm	300 2.7–4.7	300 2.7–4.4	300 2.7–5.2	300 2.7–5.7	300 2.7–5.7	300 2.7–5.7
Pile head spacing: m	14.79	18.75	20.91	14.79	18.75	20.91
Pile embedded length: m	75	73	74	80	78	79

TP, transition piece

Table 7. Key parameters of the four-leg jacket-type substructures

Return period: years	50	50	50	100	100	100
Water depth: m	27.5	35	45	27.5	35	45
Diameter of TP: cm Wall thickness: cm	653 4.2	653 4.2	653 4.5	653 4.2	653 4.5	653 4.5
Cross-section of horizontal plate girder: cm × cm Wall thickness: cm	400 × 150 4.5	400 × 150 4.5	400 × 150 4.5	400 × 150 4.5	400 × 150 4.5	400 × 150 4.5
Number of brace layers	3	3	4	3	3	4
Jacket leg batter	11	9	9	11	11	9
Diameter of jacket leg: cm Wall thickness: cm	150–250 3.5–9.0	150–250 3.5–7.2	150–250 3.0–8.5	150–250 3.5–9.0	150–250 3.5–9.0	150–250 3.5–8.5
Diameter of brace: cm Wall thickness: cm	90–100 1.6–4.0	80–100 2.0–4.5	90–110 1.4–4.5	90–100 1.8–4.0	80–100 1.9–4.5	90–110 1.4–4.5
Diameter of embedded pile: cm Wall thickness: cm	300 2.7–4.0	300 2.7–4.0	300 2.7–4.0	300 2.7–4.2	300 2.7–4.2	300 2.7–4.2
Pile head spacing: m	14.18	17.44	19.67	14.18	15.55	19.67
Pile embedded length: m	59	59	59	67	69	66

TP, transition piece

Table 8. Key parameters of the monopile-type substructures

Return period: years	50	50	50	100	100	100
Water depth: m	27.5	35	45	27.5	35	45
Diameter of TP: cm Wall thickness: cm	653–716 5.5–6.0	653–716 5.5–6.0	653–716 5.5–6.0	653–716 5.5–6.0	653–716 5.5–6.0	653–716 5.5–6.0
Diameter of MP above seabed: cm Wall thickness: cm	640–760 5.3–6.8	640–800 5.3–7.1	640–850 5.3–7.5	640–760 5.3–7.7	640–800 5.3–7.6	640–850 5.3–7.7
Diameter of embedded MP: cm Wall thickness: cm	760 6.3–8.5	800 6.7–8.5	850 7.1–9.2	760 6.3–8.5	800 6.7–8.7	850 7.1–9.2
Critical embedded pile length: m	48	50	53	49	51	53
Embedded pile length: m	48	50	53	49	51	53

TP, transition piece

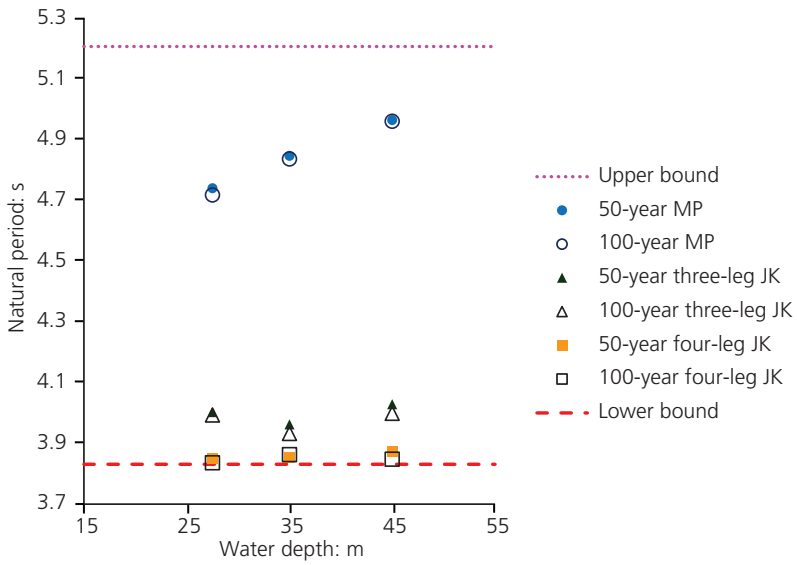

Figure 8. Natural period of the first mode shape of the overall structure in each case. MP, monopile; JK, jacket

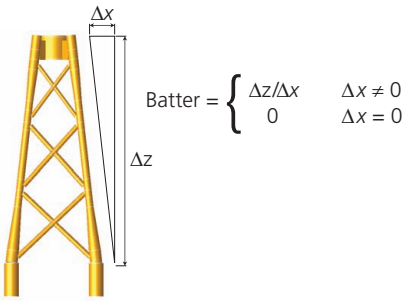

Figure 9. Definition of the batter in jackets

5.5 Weights of substructures

The water depth and weight scatter diagram of the design results is shown in Figure 10. The weights of jacket-type substructures are sensitive to the increase in the return period of storms, for storms dominate most of the members, the outer diameters and thicknesses of which are increased when the storm return period is raised from 50 to 100 years. In contrast, 100-year storms dominate the jacket piles, the lengths and thicknesses of which are increased from those of the 50-year cases. In addition, at the same water depth, a three-leg jacket is lighter than a four-leg jacket because the weight reduction due to having fewer members is greater than the weight gain due to larger sharing of the loads. Regarding the weights of monopile-type substructures, the difference in weight between the 50-year cases and the 100-year cases is not significant. This similarity is attributed to earthquakes dominating the above-seabed parts of 50-year monopiles, the thicknesses of which are slightly increased and thus capable of bearing 100-year storms. Moreover, a 20 m depth of soil liquefaction has a great impact on monopiles, the embedded parts of which are dominated by earthquakes in all cases and therefore are not sensitive to the increase in the storm return period.

Table 10. Number of members dominated by each type of load combination in four-leg jacket-type cases

Water depth: m	Number of members in 50-year return period		Number of members in 100-year return period	
	Earthquake LC	Storm LC	Earthquake LC	Storm LC
27.5	49	29	30	48
35.0	46	32	28	50
45.0	64	34	34	64

LC, load combination

Table 11. Maximum unity ratio of each case

Water depth: m	50-year three-leg JK	100-year three-leg JK	50-year four-leg JK	100-year four-leg JK	50-year MP	100-year MP
27.5	0.90	0.89	0.85	0.89	0.87	0.90
35.0	0.88	0.88	0.88	0.88	0.88	0.90
45.0	0.89	0.89	0.85	0.88	0.89	0.89

JK, jacket; MP, monopile

Table 12. Minimum fatigue life (years) of each case

Water depth: m	50-year three-leg JK	100-year three-leg JK	50-year four-leg JK	100-year four-leg JK	50-year MP	100-year MP
27.5	21.34	20.47	20.50	21.11	37.33	47.36
35.0	22.13	24.12	20.79	20.97	37.34	37.34
45.0	20.96	21.65	29.86	27.24	44.93	47.02

JK, jacket; MP, monopile

Table 9. Number of members dominated by each type of load combination in three-leg jacket-type cases

Water depth: m	Number of members in 50-year return period		Number of members in 100-year return period	
	Earthquake LC	Storm LC	Earthquake LC	Storm LC
27.5	34	25	24	35
35.0	32	27	22	37
45.0	40	34	25	49

LC, load combination

5.6 Maximum overturning moment

The maximum overturning moment can be used to evaluate the overall consequences of a structure under loading and serve as a benchmark for measuring the maximum axial load on a jacket pile or the maximum lateral displacement of the pile head of a monopile.

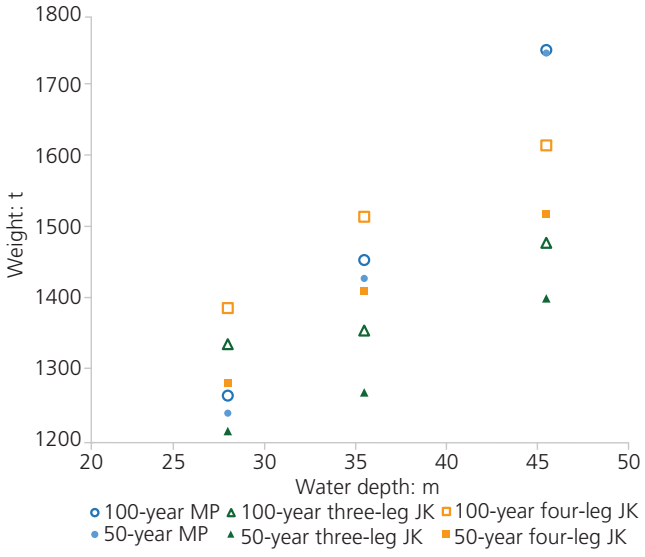

Figure 10. Water depth–weight distribution of each type of substructure in each return period. JK, jacket; MP, monopile

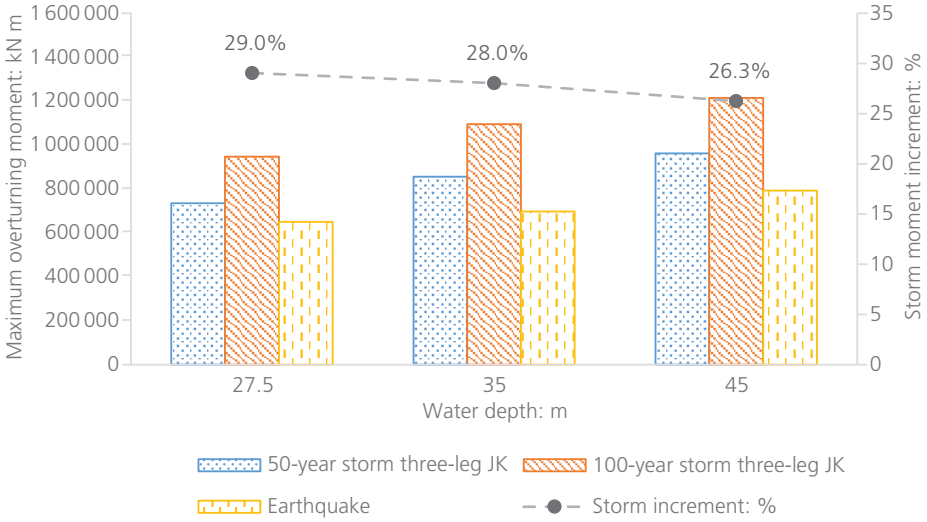

Figure 11. Maximum overturning moment of the three-leg jacket-type substructures in each return period. JK, jacket

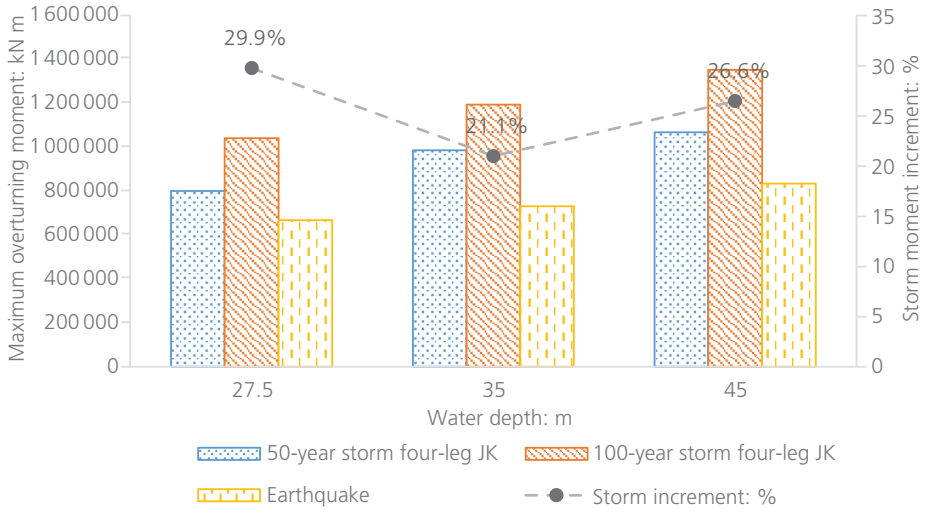

Figure 12. Maximum overturning moment of the four-leg jacket-type substructures in each return period. JK, jacket

The maximum overturning moments caused by both types of load combinations are shown in Figures 11–13. In the jacket-type cases, the maximum overturning moments induced by storms in both return periods are greater than those induced by earthquakes. These results are consistent with the prevailing dominant load combinations in the jacket members. Furthermore, the maximum overturning moment of a four-leg jacket is greater than that of a three-leg one. This may result from the fact that when a substructure has more members, greater hydraulic loads are applied to it. For monopile-type cases, the maximum overturning moments induced by both types of load combinations are close. However, in the case of a 45 m water depth, despite the maximum overturning moment of 100-year storms being less than that of earthquakes, the 100-year storms still dominate the sections of a monopile. The reason is that the critical condition of the monopile in this case is the axial force combined with bending interaction, in which the effect of axial forces should be considered as well. When the 50-year storm return period is increased to the 100-year return period, the maximum overturning moments increase by about 21.1–29.9% for jacket-type substructures and by about 20.3–26.8% for monopile-type substructures.

5.7 Embedded pile length

The design results of the embedded piles are shown in Tables 13 and 14. In general, the embedded pile length of a jacket-type substructure is dominated by the axial bearing capacity, while the embedded length of a monopile is dominated by the lateral displacement, so the critical pile length due to the displacement constraint is applied in the design. Regarding the type of critical

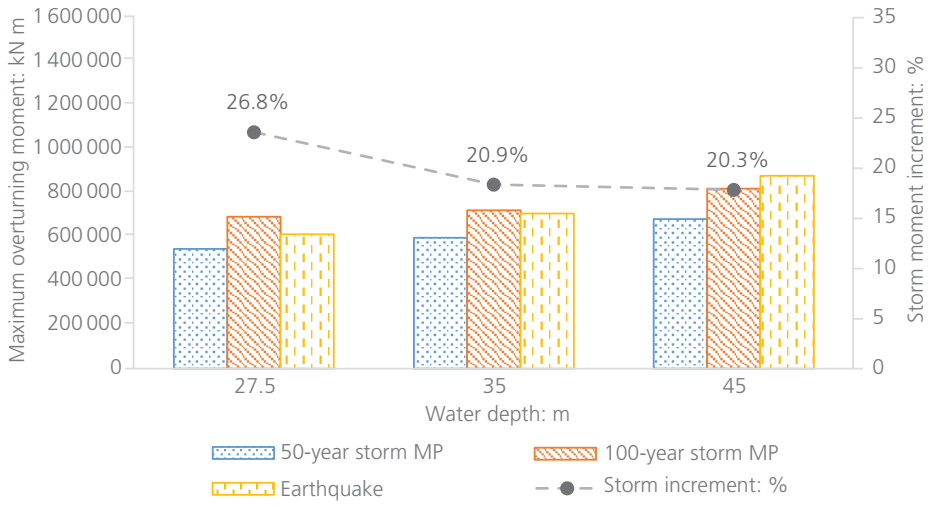

Figure 13. Maximum overturning moment of the monopile-type substructures in each return period. MP, monopile

Table 13. Design results of the embedded piles under the 50-year storm and 475-year earthquake conditions

Type	Water depth: m	Pile outer diameter: cm	Pile wall thickness: cm	Pile length: m	Critical pile length: m	Safety factor	Type of critical load
Three-leg JK (critical pile)	27.5	300	2.7–4.7	75	N/A	1.33	Earthquake
	35.0	300	2.7–4.4	73	N/A	1.35	Earthquake
	45.0	300	2.7–5.2	74	N/A	1.35	Earthquake
Four-leg JK (critical pile)	27.5	300	2.7–4.0	59	N/A	1.34	Storm
	35.0	300	2.7–4.0	59	N/A	1.32	Storm
	45.0	300	2.7–4.0	59	N/A	1.34	Storm
MP	27.5	760	6.3–8.5	48	48	1.57	Earthquake
	35.0	800	6.7–8.5	50	50	1.55	Earthquake
	45.0	850	7.1–9.2	53	53	1.52	Earthquake

JK, jacket; MP, monopile; N/A, not applicable

Table 14. Design results of the embedded piles under the 100-year storm and 475-year earthquake conditions

Type	Water depth: m	Pile outer diameter: cm	Pile wall thickness: cm	Pile length: m	Critical pile length: m	Safety factor	Type of critical load
Three-leg JK (critical pile)	27.5	300	2.7–5.7	80	N/A	1.33	Storm
	35.0	300	2.7–5.7	78	N/A	1.33	Storm
	45.0	300	2.7–5.7	79	N/A	1.35	Storm
Four-leg JK (critical pile)	27.5	300	2.7–4.2	67	N/A	1.35	Storm
	35.0	300	2.7–4.2	69	N/A	1.34	Storm
	45.0	300	2.7–4.2	66	N/A	1.34	Storm
MP	27.5	760	6.3–8.5	49	49	1.62	Earthquake
	35.0	800	6.7–8.7	51	51	1.61	Earthquake
	45.0	850	7.1–9.2	53	53	1.52	Earthquake

JK, jacket; MP, monopile; N/A, not applicable

load combinations, owing to the soil liquefaction being considered in the load combinations of earthquakes, the axial capacity and lateral resistance of the piles are reduced. Therefore, the larger maximum overturning moment due to storms may have less influence on the embedded pile length than does the reduction in pile capacity due to earthquakes. This is the reason why the piles of 50-year three-leg jackets and 100-year monopiles at water depths of 27.5 and 35.0 m are all dominated by earthquakes, even if the maximum overturning moments due to storms are greater. The safety factors of the axial load of the jacket piles are within the range 1.32–1.35, which is larger than 1.30, and those of the monopiles are in the range 1.52–1.62, which still have considerable margins when the lateral displacement constraint is met.

6. Conclusions

The jacket-type (three-leg and four-leg) and monopile-type substructures are taken into account to evaluate the influence of typhoons on offshore wind turbine foundations under different water depth conditions. The typhoon impact is considered to increase the design criteria for wind, waves and currents from a 50-year return period to a 100-year return period. Under the basic conditions of the site-specific soil properties and the design response spectrum of a certain wind farm in an area offshore of Changhua County in central Taiwan, the conclusions of the substructure design results can be summarised as follows.

- The overall geometry of an offshore WTG substructure is neither dominated by the allowable range of natural periods nor sensitive to the increase in a return period in the ULS. However, the size and thickness of an individual member are dominated by the ULS.
- Increasing the storm return period from 50 to 100 years has a significant influence on members that continue to be dominated by storms rather than on those that were previously dominated by earthquakes.
- The influence of different storm return periods on environmental loads is evaluated by maximum overturning moments at the seabed level. When the 50-year storm return period is increased to the 100-year return period, the maximum overturning moments are increased by 21.1–29.9% for jacket-type substructures and by 20.3–26.8% for monopile-type substructures.
- The results of structural weights show that increasing the storm return period has a great impact on jacket-type substructures, particularly on their piles, the lengths of which need to be increased to bear axial loads due to enhanced maximum overturning moments.
- In this study, the three-leg jackets provided more benefits than four-leg jackets in the form of less weight and smaller maximum overturning moments under the same environmental conditions. If the construction and the installation phases are considered, the additional benefits, such as less welding work and shorter installation times, will result in the three-leg jackets being more economical.

REFERENCES

ABS (American Bureau of Shipping) (2018) *Bottom-founded Offshore Wind Turbine Installations*. ABS, Houston, TX, USA.
API (American Petroleum Institute) (2014a) API RP 2MET: Derivation of metocean design and operating conditions. API, Washington, DC, USA.
API (2014b) API RP 2GEO: Geotechnical and foundation design considerations. API, Washington, DC, USA.
ASTM (2011) E 1049–85: Standard practices for cycle counting in fatigue analysis. ASTM International, West Conshohocken, PA, USA.
CWB (Central Weather Bureau) (2019) *Categorized Paths of Typhoons Invading Taiwan*. CWB, Taipei, Taiwan. See https://www.cwb.gov.tw/V7e/knowledge/encyclopedia/ty017.htm (accessed 27/08/2019).
DNV GL (Det Norske Veritas & Germanischer Lloyd AS) (2016a) DNVGL-ST-0126: Support structures for wind turbines. DNV GL, Oslo, Norway.
DNV GL (2016b) DNVGL-ST-0437: Loads and site conditions for wind turbines. DNV GL, Oslo, Norway.
DNV GL (2016c) DNVGL-RP-0416: Corrosion protection for wind turbines. DNV GL, Oslo, Norway.
DNV GL (2016d) DNVGL-RP-C203: Fatigue design of offshore steel structures. DNV GL, Oslo, Norway.
F3WP PO (Formosa III Wind Power Co. Ltd. Preparatory Office) (2018) *Formosa III Offshore Wind Power Project: Wind Farm No. 1 Environmental Impact Statement*. F3WP PO, Taipei, Taiwan.
IEC (International Electrotechnical Commission) (2005) IEC 61400-1:2005: Wind turbines – Part 1: Design requirements. IEC, Geneva, Switzerland.
IEC (2009) IEC 61400-3:2009: Wind turbines – Part 3: Design requirements for offshore wind turbines. IEC, Geneva, Switzerland.
Standards Norway (2013) NORSOK N-004: Design of steel structures. Standards Norway, Lysaker, Norway.
Stocker TF, Qin D, Plattner GK *et al.* (2013) *Climate Change 2013: the Physical Science Basis. Contribution of Working Group I to the Fifth Assessment Report of the Intergovernmental Panel on Climate Change*. Cambridge University Press, Cambridge, UK; New York, NY, USA.